

## Preparation and characterisation of edible layer-by-layer coatings of sodium polyacrylate/chitosan for the preservation of strawberries

Long, M., Tao, S.-K., Wang, X.-H., Wang, J.-Y., Hu, Y.-Y., Cai, H.-Z. and \*Zhan, G.

College of Biological and Food Engineering, Chuzhou University, Chuzhou 239000, China

### Article history

Received: 16 January 2020

Received in revised form:

21 July 2020

Accepted:

8 September 2020

### Abstract

To improve the preservation of strawberries during storage, an edible coating was prepared using a layer-by-layer self-assembly electrostatic deposition technology. Sodium polyacrylate (PAAS) was used as polyanion solution, and chitosan (CS) was used as polycation solution. The obtained coating was characterised to determine its self-repairing ability and its effect on the preservation of strawberries. The results showed that CS (9 mg/mL) and PAAS (5 mg/mL) could assemble, by hydrogen and ionic bonding, to form a new coating with no obvious pores and had a tight cross-sectional structure. The PAAS/CS self-assembled coating displayed high water resistance (water vapor transmission rate,  $31.22 \times 10^{-11} \text{ g} \cdot \text{m}^2 \cdot \text{s} \cdot \text{Pa}^{-1}$ ), transparency (light transmittance, 87.5%), and excellent mechanical properties (tensile strength, 17.31 MPa; elongation at break, 13.72%). The self-repairing ability of the PAAS/CS coating upon scratching was manifested by the repair of the coating's morphology (repair rate, 81.05%), and the restoration of its mechanical properties. When compared with uncoated strawberries, PAAS/CS coating significantly reduced the weight loss rate, the rot rate during storage ( $p < 0.05$ ), and the loss of anthocyanin and vitamin C. In conclusion, the PAAS/CS coating greatly improved the fresh-keeping of strawberries.

© All Rights Reserved

### Keywords

layer-by-layer  
self-assembly,  
edible coating,  
self-repairing,  
structural characteriza-  
tion,  
strawberry preservation

### Introduction

With the increasing variety and application range of edible coatings, many studies have shown that these coatings can effectively regulate the exchange of moisture, gas, and organic volatile substances between fruits and their external environment (Nottagh *et al.*, 2018). This has greatly extended the preservation time of fruits (Xu *et al.*, 2001; Sun *et al.*, 2010). For example, Marelli *et al.* (2016) dip-coated a silk fibroin solution on the surface of strawberries, and found that the respiration and weight loss rate were significantly decreased ( $p < 0.05$ ), which extended their shelf life. However, with the increasing requirements for food preservation in the consumer market, the development of multifunctional composite coatings has become a hot research topic (Nottagh *et al.*, 2019; Fasihnia *et al.*, 2018a). González Sandoval *et al.* (2019) formulated edible films using organic mucilage from *Opuntia ficus-indica* and pectin. Fasihnia *et al.* (2018b) developed PP based antimicrobial packaging films containing sorbic acid for food applications. The type of functional packaging and coating can significantly improve the preservation of fruits and vegetables (Sakooei-Vayghan *et al.*, 2019).

The layer-by-layer self-assembly is a technique using different polyelectrolytes, by taking

advantage of the electrostatic attraction between oppositely charged molecules (Yang *et al.*, 2017). The self-assembly process can be achieved by electrostatic forces, hydrogen bonds, Van Der Waals forces, and other between differently charged molecules, and there are no new covalent bonds generated (Jiang *et al.*, 2016; Zhao *et al.*, 2019). Therefore, the thickness and distribution uniformity of the coating can be adjusted by varying several parameters, including the concentration of the polyelectrolyte solution, the number of assembly time, the ion concentration, and the pH value. These characteristics can be used to prepare a multi-functional coating with controllable water-blocking, gas barrier, and antibacterial and antioxidant properties (Ugur *et al.*, 2016; Li *et al.*, 2018). In addition, functional coatings formed by self-assembly of reversible and weak intermolecular non-covalent bonds also have the ability to self-repair after local damage (Wang *et al.*, 2017). This function can restore its original toughness, tensile strength, surface smoothness, and other properties; and has become a hot topic in academic research both in China and abroad (Hou *et al.*, 2016; Pinto *et al.*, 2017). Edible self-repairing coatings can be divided into spontaneous and non-spontaneous repairing coatings based on their self-repairing process. Spontaneous repairs are achieved through the interaction of molecules intrinsic

\*Corresponding author.  
Email: [zhangezcxy@163.com](mailto:zhangezcxy@163.com)

to the coating, while non-spontaneous repairs require interventions including light, heat, pH changes, and etc. (Zhao *et al.*, 2016; Kumarasamy *et al.*, 2018). In addition, according to the self-repairing mechanism of the coating, it can be achieved by non-covalent bond forces such as intermolecular hydrogen bonds, and multiple repairs can be achieved as well (Wang and Zhou, 2018).

Sodium polyacrylate (PAAS) is a common anionic polyelectrolyte with strong thickening ability and excellent water retention. An aqueous solution of PAAS is extremely stable, odourless, tasteless, long-lasting, easy to store, and harmless to the human body. It is a food additive approved by the FDA and the Chinese Ministry of Health for use in pasta, processed foods, and frozen foods (Kim *et al.*, 2017). The carboxylic groups in PAAS contribute a large negative charge in the molecular chain, thus turning its aqueous solution into a fully ionised anionic polyelectrolyte; allowing the binding of a large number of cations through electrostatic attraction (Falk *et al.*, 2001). CS is a typical positively charged polymer material. Under acidic conditions,  $-NH_2$  in chitosan can be converted to  $-NH_3^+$ , which can form self-assembled coatings with anionic polyelectrolytes (Helander *et al.*, 2001). For example, Abugoch *et al.* (2015) prepared an edible coating using the electrostatic attraction between CS and quinoa protein, which delayed the maturation process of blueberries. Arnon *et al.* (2015) formed edible coatings on the surface of oranges using layer-by-layer self-assembly of carboxymethyl cellulose (CMC) and CS, and showed that the CMC/CS coating effectively improved the preservation of the oranges. In the present work, we used PAAS as a polyanion solution and CS as a polycation solution to prepare an edible preservation coating using layer-by-layer self-assembly electrostatic deposition technology, and then characterised and analysed its structure, mechanical properties, and self-repairing ability. Moreover, we also studied the effect of PAAS/CS coating on the preservation time of strawberries.

## Materials and methods

### Materials

Strawberries were collected in JuRong, JiangSu province, China. The fruits (weight  $20 \pm 2$  g) were of uniform maturity (80% matured) without mechanical damage, and free of pests and diseases. Following post-cold treatment, the strawberries were immediately transported to the laboratory. PAAS (food grade) was purchased from Zhengzhou Xuequan Electronics Co., Ltd.; CS and  $CaCl_2$  were purchased

from Sinopharm Chemical Reagent Co., Ltd.; *Staphylococcus aureus* CMCC (B)26003, *Escherichia coli* ATCC 25922), *Salmonella* Typhimurium ATCC 14028, and *Listeria monocytogenes* ATCC 19111 were purchased from Guangdong Huankai Microbiology Technology Co., Ltd. Other reagents were analytically pure, and purchased from Sigma or Sinopharm Chemical Reagent Co., Ltd.

### Methods

#### Preparation of the coating

To prepare the polycationic solution, CS powder was mixed with 98 mL distilled water and 2 mL  $CH_3COOH$  (1%, w/w) at  $55^\circ C$  for 6 h using a magnetic stirrer at 300 rpm. Then,  $CaCl_2$  (30%, 4 mg/mL) was added to the CS solution, stirred evenly with a glass rod, and allowed to stand for 30 min. In addition, PAAS at various concentrations was prepared as a polyanionic solution. A glass slide was lowered into the polyanionic solution for 5 min, after which the excess electrolyte molecules on the surface were washed with distilled water. Subsequently, this glass slide was immersed in the polycationic solution for 5 min. The polyanionic and polycationic solution were adsorbed and assembled by electrostatic interaction, and a combination of polyanionic and polycationic electrolyte was formed on the slide, that is, one layer of PAAS/CS coating. Multiple coatings were obtained by repeating the above steps, and three layers of coatings were prepared in the present work (Ugur *et al.*, 2016). The prepared coating was dried at  $60^\circ C$  for 12 h in an oven, and then placed at  $23^\circ C$  with 50% relative humidity.

#### Effect of different CS or PAAS concentrations on the properties of the PAAS/CS coating

To study the effect of varying the CS concentration on the properties of the PAAS/CS coating, different PAAS/CS coatings were prepared by keeping the PAAS concentration fixed at 5 mg/mL, and varying CS concentrations at 6, 7, 8, 9, and 10 mg/mL. To study the effect of varying the PAAS concentration on PAAS/CS coating, different PAAS/CS coatings were prepared by keeping the CS concentration fixed at 9 mg/mL, and varying the PAAS concentrations at 3, 4, 5, 6, and 7 mg/mL. We then assessed the gas permeability ( $O_2$  and  $CO_2$ ), water vapor permeability (WVP), water solubility (WS), and light transmittance of the different PAAS/CS coatings.

#### Structural characterisation of PAAS/CS coatings

To characterise the microstructure of film surface, small strips ( $5 \times 5$  mm) of the PAAS/CS films were mounted on aluminium stubs, coated with a thin

layer of gold, and observed using a Scanning Electron Microscope (Philips: XL30, model: KYKY-EM3200, China), at an accelerating voltage of 25 kV (Falk *et al.*, 2001).

To analyse the PAAS/CS films by Fourier transform infrared (FTIR) spectroscopy, 2 mg of the sample were ground, and compressed with 200 mg KBr. The FTIR spectrum was obtained at 20°C, at the range of 500 - 4000 cm<sup>-1</sup> using an FTIR-430 (Jascow, Japan) (Helander *et al.*, 2001).

#### *Performance characterisation of PAAS/CS coating*

To determine the mechanical properties of PAAS/CS coatings, film specimens were cut into rectangular shapes of 2.5 × 5 cm. The tensile strength (TS) and elongation at break (E) of the films were determined using an Instron Universal Testing Machine (Model 5566, Instron Engineering Corporation, Canton, MA) with 50 N load cell following the ASTM-D882-02 standard method (ASTM, 2002). The initial gauge separation and the crosshead speed were set at 50 mm and 5 mm/min, respectively. TS characterised the mechanical strength of the coating, and E was the maximum strain value at which the coating was broken, which characterised the elasticity of the coating.

To determine the antimicrobial effect of the films, four pathogenic bacteria (*St. aureus*, *E. coli*, *Sal. Typhimurium*, and *L. monocytogenes*) were inoculated onto nutrient broth medium, cultured in a constant temperature shaker at 37°C for 24 h, and then collected by centrifugation at 7,000 rpm and 4°C for 7 min. The bacteria were resuspended with normal saline, and diluted to a concentration of 10<sup>5</sup>~10<sup>6</sup> CFU/mL. Then a UV-sterilised PAAS/CS coating (1 g) was added to 1 mL of the above-mentioned bacterial cultures, and cultured at 37°C for 12 h. The solutions without PAAS/CS coating served as control. The bactericidal effect of the PAAS/CS coating was determined by plate counting using Eq. 1

$$\text{Sterilization rate} = M_1/M_0 \times 100\% \quad (\text{Eq. 1})$$

where,  $M_1$  = number of colonies after treatment with PAAS/CS (CFU/g), and  $M_0$  = number of colonies before treatment (CFU/g) with PAAS/CS.

#### *Self-repairing ability of the PAAS/CS coating*

A clean surgical blade was used to scratch the shape of “×” penetrating the coating. Next, the “×” was covered with ultra-pure water using a syringe. Then, the healing process of the scratched coating was observed. After 30 min, the healing state of the coating was recorded to evaluate the self-repairing ability of

the coating (Wang and Zhou, 2018).

Three pieces of PAAS/CS coatings were prepared. One coating was stained with Rhodamine B for 10 min. After staining, the coating was dried in an oven at 60°C, and completely removed from the slide by a utility knife. The ends of the coatings of different colours overlapped (by about 1 cm) so that the two coatings were in contact with each other. The overlapping portions were lightly pressed, and ultrapure water was added, and the coatings were allowed to merge at room temperature for 30 min. The self-repairing ability of the two coatings was investigated by separately measuring their mechanical properties. The ratio of the tensile strength before and after the repairing of the coating was taken as the repairing rate of the coating (Wang and Zhou, 2018).

#### *Effect of PAAS/CS coating on the fresh-keeping of strawberries*

In order to remove residual pesticides, dust, and other debris from the surface of the strawberries, the surface of the strawberries was washed with water. After being placed at 25 ± 2°C for 30 min, the preservation coating was applied as follows:

- i) The pre-treated strawberries were randomly divided into two groups. The experimental group was treated with PAAS/CS coatings, and the control group was not treated.
- ii) The strawberries of the experimental group were first immersed in a PAAS solution (5 mg/mL) for 5 min, and air-dried at 25 ± 2°C for 10 min. Then, the strawberries were completely immersed in a CS solution (9 mg/mL) for 5 min, and then air-dried at 25 ± 2°C for 10 min. A layer of PAAS/CS coating was formed on the surface of the strawberry upon completion of this step.
- iii) Step (ii) was repeated twice to form a total of three layers of PAAS/CS coating on the surface of the strawberries.
- iv) The uncoated control group and the PAAS/CS-coated strawberries were stored in a constant temperature and humidity equipment at 25°C and 60% RH. Then the weight loss rate, rot rate, and changes in vitamin C and anthocyanin contents of the strawberries were measured after 0, 1, 3, 5, and 7 days.

#### *Test methods*

The water vapour permeability (WVP) was determined using a modification of the ASTM E96 (ASTM, 1995). The gravimetric method was used to

determine the relative humidity (RH) at the film underside. One sample without defects was cut from each PAAS/CS coating. Samples were conditioned for 48 h in a chamber at 25°C and 50% RH before being analysed. Distilled water (6 mL) was dispensed into cups with wide rims. The rim of each cup was coated with silicon sealant. The PAAS/CS coating was sealed to the base of the cup with a ring using a rubber band. The cups were placed at 25°C and 50% RH in a desiccator. The weight of the cups was measured at 1 h intervals for 9 h. Simple linear regression was used to estimate the slope ( $G$ ) of weight loss vs. time. Eq. 2 was used to calculate the WVP.

$$\text{WVP} = \frac{G \cdot x}{A \cdot \Delta p} \quad (\text{Eq. 2})$$

where,  $x$  = film thickness (mm),  $A$  = area of exposed PAAS/CS coating (m<sup>2</sup>),  $\Delta p$  = difference in partial WVP (kPa) between the two sides of the coating.

The water solubility (WS) was determined as follows: PAAS/CS coatings were cut into pieces of 2 × 2 cm, dried in an oven at 105°C for 2 h, and the weight accurately recorded as  $M_1$ . The coating was placed in a beaker containing 30 mL of distilled water, and slightly shaken for 24 h. Then the coating was dried in an oven at 105°C for 2 h, and its weight recorded as  $M_2$  (Hoque *et al.*, 2011). The WS was calculated using Eq. 3:

$$\text{WS} = \frac{M_1 - M_2}{M_1} \quad (\text{Eq. 3})$$

Oxygen and carbon dioxide permeability measurements were carried out with a Labthink VAC-V2 following the differential-pressure method described by GB/T 1038-2000 (China Quality and Technical Supervision, 2000). Samples (in the shape of a circle, 97 mm diameter) without defects were cut from each PAAS/CS coating. Samples were conditioned for 48 h in a chamber at 25°C and 50% RH before being analysed. A temperature of 25°C and RH of 50% were selected as experimental conditions, while the ambient temperature of the test centre was 23.3°C, and the RH was 49%. Each pre-treated sample was placed between the upper and lower test chambers, and clamped. First, a vacuum was applied to the lower chamber, and then a vacuum was applied to the whole system (to below 27 Pa). Next, the upper testing chamber (higher pressure chamber) was filled with the testing gas at a specific and constant pressure differential between upper and lower testing chambers. Due to the pressure

differentials, the testing gas penetrated from the higher pressure chamber into the lower pressure chamber. Pressure differentials ( $\Delta p$ ) of the lower pressure chamber were recorded, and the testing time ( $t$ ) was taken until the pressure differential remained constant in the same time intervals due to a constant permeation of the testing gas. The pressure differentials of three successive time intervals were selected to calculate the arithmetic mean ( $\Delta p/\Delta t$ ). Eq. 4 was used to calculate gas transmission ( $Q_g$ ):

$$Q_g = \frac{\Delta p}{\Delta t} \times \frac{V}{S} \times \frac{T_0}{P_0 T} \times \frac{24}{p_1 - p_2} \quad (\text{Eq. 4})$$

where,  $Q_g$  = gas transmission (cm<sup>3</sup>/m<sup>2</sup>·d·Pa);  $\Delta p/\Delta t$  = arithmetic mean of the pressure differentials of the lower pressure chamber in unit time, when the testing gas is stably permeated (Pa/s);  $V$  = volume of the lower pressure chamber (cm<sup>3</sup>);  $S$  = area of the sample (m<sup>2</sup>);  $T$  = testing temperature (K);  $p_1 - p_2$  = pressure differential between the upper and lower testing chambers (Pa);  $T_0$  = temperature in its standard state (273.15 K); and  $p_0$  = pressure in its standard state (1.0133 × 10<sup>5</sup> Pa).

The weight loss rate of the sample during storage was calculated using Eq. 5 (Arifin *et al.*, 2013):

$$\text{Weight Loss rate (\%)} = \frac{M_1 - M_2}{M_1} \times 100 \quad (\text{Eq. 5})$$

where,  $M_1$  = initial mass, and  $M_2$  = mass after storage.

Fruit decay was calculated using Eq. 6 (Widiastuti *et al.*, 2013)

$$\text{Fruit Decay (\%)} = \frac{\text{Num. of fruit decay}}{\text{Total fruit}} \times 100 \quad (\text{Eq. 6})$$

Anthocyanin and vitamin C contents were determined as follows: a sample of whole strawberries (approximately 25 g) was homogenised in 10 volumes of a cold solution of 3% (w/v) metaphosphoric acid and 8% glacial acetic acid (v/v) in water (pH 1.5) for 1 min, using a Waring Blender. A uniform suspension of the homogenate was stored at -70°C for anthocyanin and vitamin C analyses (Buchweitz *et al.*, 2013).

Anthocyanin was extracted and isolated as previously described (Buchweitz *et al.*, 2013) with a simple modification, *i.e.*, using 10 mL of a sample and 20 mL of 30% (by volume) aqueous ethanol. The mixture was extracted for 30 min at 70°C in an

ultrasonic bath, filtered through Whatman No. 4 filter paper (Whatman International Ltd., Kent, UK) using a funnel into a volumetric flask. The filtrate was adjusted to 50 mL in a volumetric flask with 30% aqueous ethanol.

The total anthocyanin content (TAC) was determined by the pH-differential method (Lee *et al.*, 2005). Briefly, 1 mL extracted solution was transferred into a 10 mL volumetric flask for preparing two dilutions of the sample; one, the volume was adjusted with potassium chloride buffer, pH 1.0, and the other one with sodium acetate buffer, pH 4.5. The dilutions were equilibrated for 15 min. The absorbance of each dilution was measured at 518 and 700 nm, against a blank cell filled with distilled water. The absorbance of the diluted sample ( $\Delta A$ ) was calculated using Eq. 7:

$$\Delta A = (A_{518\text{nm}/\text{pH}1.0} - A_{700\text{nm}/\text{pH}1.0}) - (A_{518\text{nm}/\text{pH}4.5} - A_{700\text{nm}/\text{pH}4.5}) \quad (\text{Eq. 7})$$

The monomeric anthocyanin pigment concentration in the original sample was calculated using Eq. 8, and was converted to mg of total anthocyanin content/100 g sample:

$$\text{Monomeric anthocyanin pigment (mg/L)} = \frac{\Delta A \times MW \times DF \times 1000}{\epsilon \times l} \quad (\text{Eq. 8})$$

where, MW = molecular weight, DF = dilution factor, and  $\epsilon$  = molar absorptivity. The pigment content was calculated as cyanidin-3-glucoside, where MW = 449.2 and  $\epsilon$  = 26,900.

The vitamin C content of the strawberries was analysed by HPLC (Odrizola *et al.*, 2008). A sample of strawberry homogenate (25 g) was mixed with 25 mL of a solution containing 45 g of metaphosphoric acid and 7.2 g of DL-1,4-dithiothreitol per litre. The mixture was centrifuged at 12,000 rpm for 15 min at 4°C. The supernatant was passed through a Millipore membrane (0.45  $\mu\text{m}$ ). An aliquot of 20  $\mu\text{L}$  was injected into the HPLC system using a reverse-phase C18 Spherisorb® ODS2 (5  $\mu\text{m}$ ) stainless-steel column (4.6 mm  $\times$  250 cm). The mobile phase was a 0.01% solution of sulphuric acid adjusted to pH 2.6. The flow rate was fixed at 1.0 mL/min at 20°C. Detection was performed at 245 nm. The results were expressed as milligrams of vitamin C per 100 g of strawberries.

#### Statistical analysis

All experiments were performed in

triplicates unless otherwise stated. The means and standard deviations (SD) were calculated using Microsoft Excel software. LSD (Least Significant Difference) method was used to compare the differences among means at the level of 0.05 using the SAS 9.2 software ( $X \pm \text{SDV}$ ,  $n = 3$ ).

## Results and discussion

### *Effect of polyelectrolyte concentration on the barrier property of PAAS/CS coatings*

#### *Effect of PAAS concentration on the barrier property of PAAS/CS coatings*

Figure 1(a) and 1(b) show the barrier property of PAAS/CS coating samples produced with different concentrations of PAAS. With the increase in PAAS concentration, WS and WVP of the coating significantly decreased ( $p < 0.05$ ), which indicated that the water resistance of the coating continuously improved (Figure 1(a)). In addition, when the amount of PAAS was 5~7 mg/mL, WS of the coating did not significantly change any further with the increase in PAAS concentration ( $p > 0.05$ ). When the amount of PAAS was 3~5 mg/mL, the gas permeability significantly decreased ( $p < 0.05$ ) as compared to control. However, as the concentration of PAAS increased further, the oxygen and carbon dioxide permeability started to increase, which meant that the gas permeability of the coating gradually increased. This result indicated that an excessive polyanion concentration is not conducive to the barrier property of the PAAS/CS coating, that is, when the PAAS concentration is 5 mg/mL, the barrier property of the coating was optimal.

#### *Effect of CS on the barrier property of PAAS/CS coatings*

Figure 1(c) and 1(d) show the water resistance of PAAS/CS coating samples that were incorporated with different amounts of CS. When the amount of CS increased to 9 mg/mL, both WS and WVP of the coating were significantly reduced ( $p < 0.05$ ), which indicated that an increase in CS concentration had a positive effect on improving the water resistance of PAAS/CS coating in this concentration range. However, as the CS concentration continued to increase to 10 mg/mL, there was only a slight further reduction of WS and WVP ( $p > 0.05$ ). In addition, Figure 1(d) shows that when the concentration of CS used was between 6~9 mg/mL, the gas permeability ( $\text{O}_2$  and  $\text{CO}_2$ ) of the coating significantly decreased ( $p < 0.05$ ). As the concentration of CS continued to increase, the permeability of both  $\text{O}_2$  and  $\text{CO}_2$  significantly

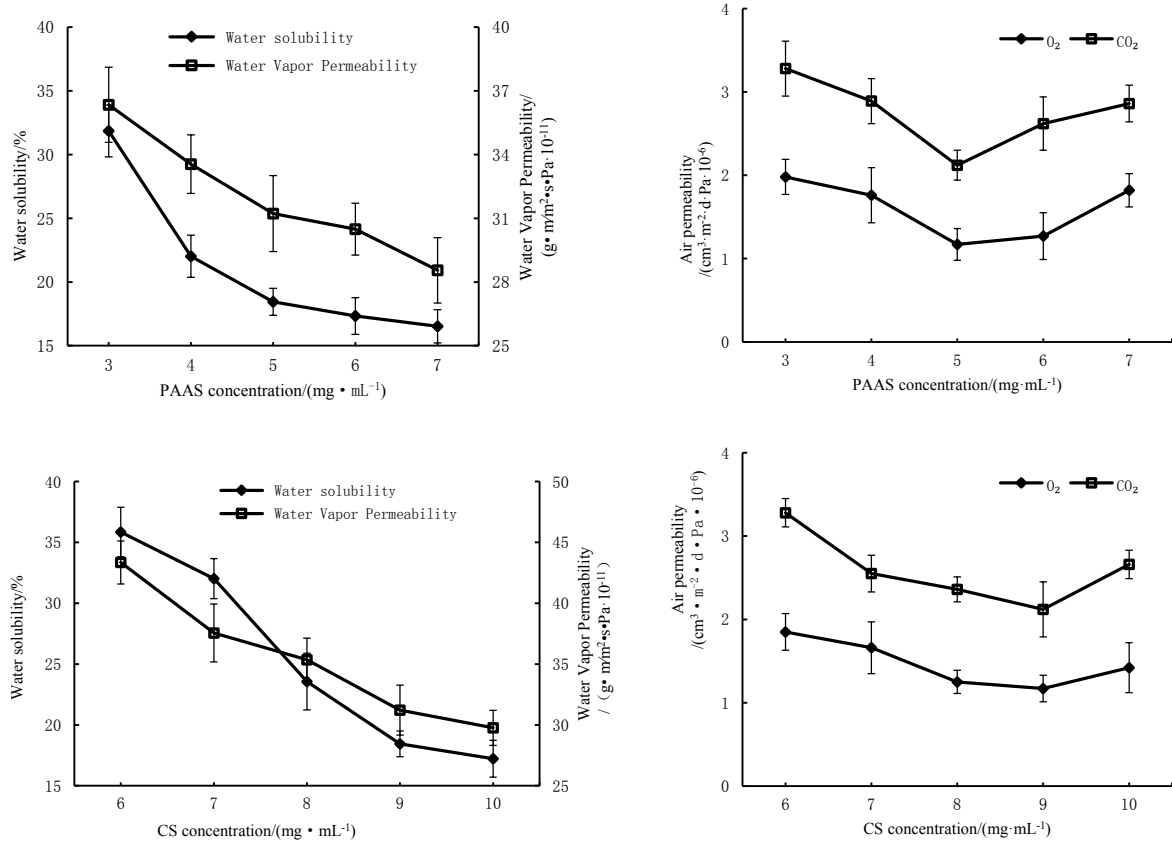


Figure 1. Effect of PAAS and CS concentration on the barrier properties of PAAS/CS coating. (a) and (b): water-resisting properties; (c) and (d): air permeability.

increased. In addition, it can be seen from Figure 1(d) that when the concentration of CS was 6~9 mg/mL, the gas permeability (O<sub>2</sub> and CO<sub>2</sub>) of the coating significantly decreased ( $P < 0.05$ ). As the concentration of CS continued to increase, the permeability of both O<sub>2</sub> and CO<sub>2</sub> significantly increased. This is probably due to the high concentration of CS, accumulating too much of the polycation solution on the polyanion layer, which affected the flatness and barrier property of the coating (Xu *et al.*, 2001). Hence, the optimal barrier property of PAAS/CS coating occurred when the concentration of CS was 9 mg/mL.

#### Effect of polyelectrolyte concentration on light transmittance of PAAS/CS coating

The light transmittance of the coating is an important indicator for evaluating the quality of self-assembled coatings, mainly because it is not only an aid to evaluate the compatibility of the two polyelectrolytes, but also an important indicator to evaluate the applicability of the coating to food surfaces (Widiastuti *et al.*, 2013). When the light transmittance of the coating is too low, the inherent colour of the food surface is blocked. Figure 2 shows the effect of different polyelectrolyte concentrations

on light transmittance of the PAAS/CS coating. As the PAAS or CS concentrations increased, the light transmittance of the coating gradually decreased. When the PAAS concentration was increased to 5 mg/mL, the transmittance of the coating reached 87.5%. At this time, the coating had a good transparency. But as the PAAS concentration continued to increase, the transmittance of the coating drastically decreased (Figure 2(a)). In addition, when the CS concentration was greater than 9 mg/mL, the transmittance of the coating was also significantly reduced. Therefore, in terms of light transmittance, the optimal concentration of PAAS was 5 mg/mL and that of CS was 9 mg/mL, giving the PAAS/CS coating a higher transparency, which was more suitable for the preservation of fruits.

#### Structural characteristics of PAAS/CS coating Scanning electron microscopy

In view of the above results, we prepared a PAAS/CS coating using 5 mg/mL PAAS and 9 mg/mL CS. Figure 3(A)-(a) shows scanning electron microscopy (SEM) results of its surface and cross section. CS and PAAS were evenly distributed and formed a relatively flat coating, but some small bulges can be seen on the surface. In addition, Figure

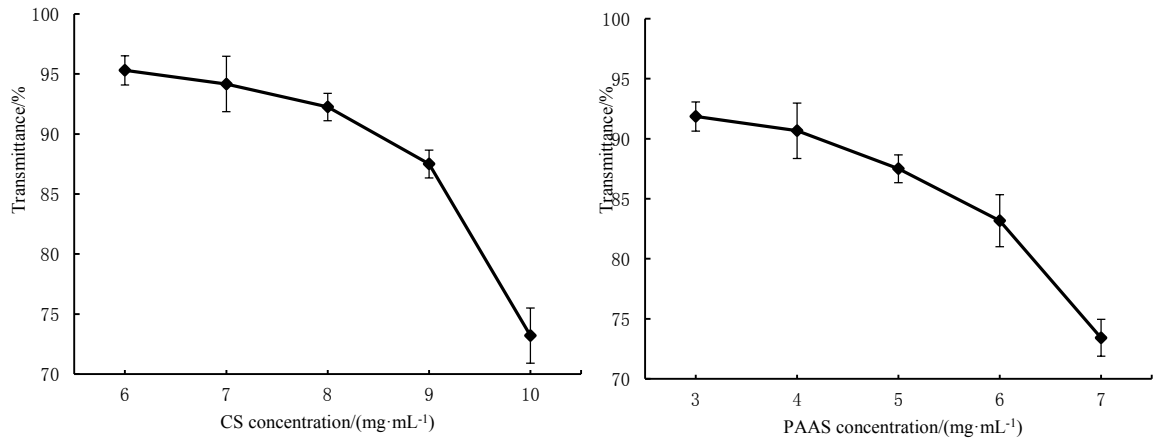


Figure 2. Effect of polyelectrolyte concentrations on light transmittance by PAAS/CS coating. (a) PAAS concentration, and (b) CS concentration.

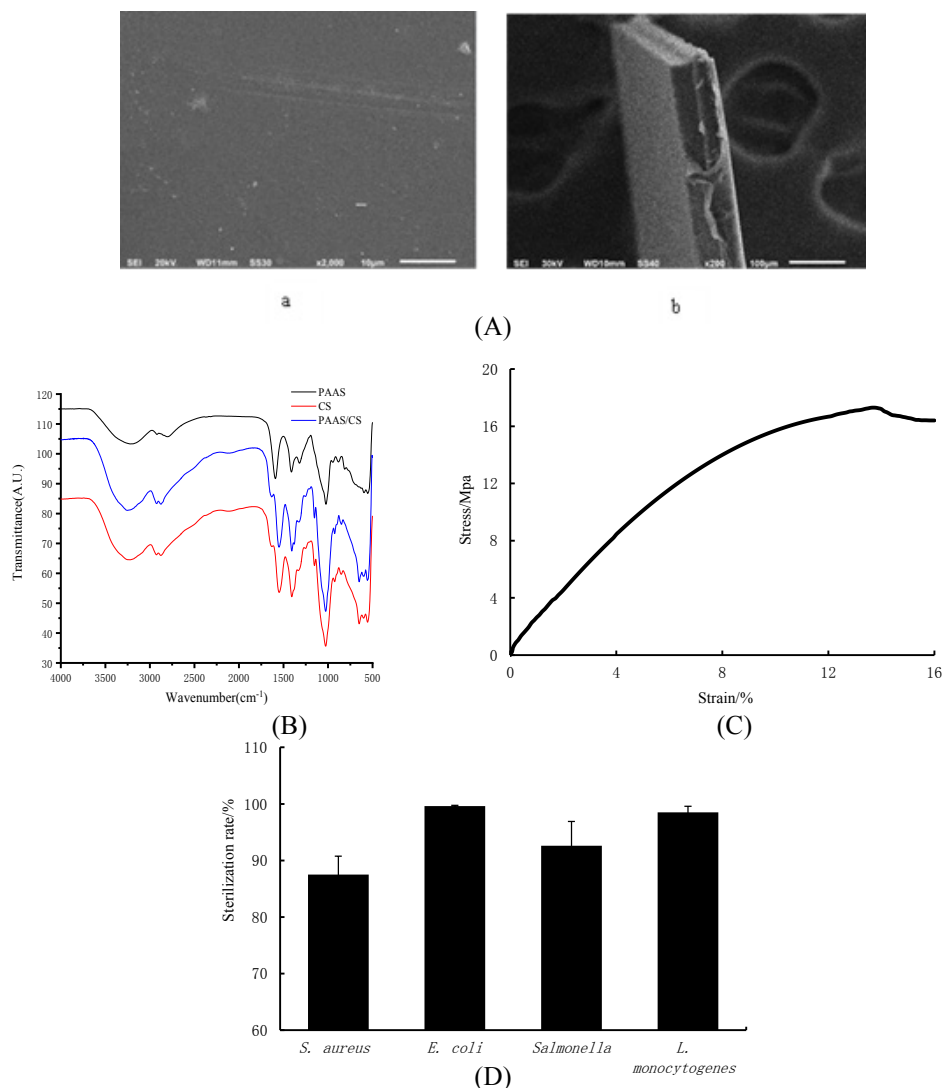


Figure 3. Structural characteristics of PAAS/CS. (A) PAAS/CS coating scanning electron microscope results, (B) Infrared spectrum of PAAS/CS at 4000-500 cm<sup>-1</sup>, (C) Stress-strain curve of PAAS/CS coating, and (D) The bactericidal effect of PAAS/CS coating. Note: (a) SEM of surface, and (b) SEM of cross-section.

3(A)-(b) shows that there was no obvious pore structure in the coating, which indicated that the cross-sectional structure was relatively tight.

*Fourier transform infrared (FT-IR) spectroscopy*

We next analysed the PAAS/CS coating using Fourier transform infrared (FT-IR)

spectroscopy. Figure 3(B) shows that the FT-IR spectrum displayed a wide -OH peak in the PAAS/CS coating near  $3267\text{ cm}^{-1}$ , and a characteristic peak of C-O-NHR was seen at  $1555\text{ cm}^{-1}$ , which was mainly linked to remaining residual acetyl groups in CS. Additionally, the PAAS spectrum showed an asymmetric vibration peak of -C=O- at  $1407\text{ cm}^{-1}$ , and no new feature peaks appeared in PAAS/CS coating. Comparison of the FT-IR spectra of CS, PAAS, and the PAAS/CS coating revealed that no new covalent bonds were formed between PAAS and CS, and that they were linked by hydrogen and ion bonds.

#### Mechanical properties of PAAS/CS coating

Tensile strength (TS) is usually used to characterise the overall strain capacity of coatings. The larger the TS, the stronger the mechanical properties of coatings, and the better they are able to withstand external tension, collision, and other stresses. Elongation at break (EAB) is used to characterise the elasticity of the coating. The larger the EAB, the better the plasticity of the coating, which means that coatings with a larger EAB value tend to adhere to the surface of the fruit and deform as the surface of the fruit changes. Figure 3(C) shows the stress-strain curve of a PAAS/CS coating (formed by combining PAAS at  $5\text{ mg/mL}$  and CS at  $9\text{ mg/mL}$ ). The stress value at the highest point in the curve is the TS, and the corresponding strain value is the EAB of the PAAS/CS coating. Therefore, the TS of the PAAS/CS coating was  $17.31\text{ MPa}$ , and the corresponding EAB was  $13.72\%$ . Previously, Liu *et al.* (2016) concluded that the TS and EAB of PAAS/CS coating were  $12.90\text{ MPa}$  and  $26.87\%$ , respectively. The difference between their results and ours is probably due to the difference in polyelectrolyte concentrations and polycations. In addition, when compared with the CMC/CS coating prepared by Zhang *et al.* (2009) (TS value of  $34.44\text{ MPa}$ , EAB value of  $6.85\%$ ), the TS of our PAAS/CS coating was lower, while the EAB was significantly higher ( $p < 0.05$ ), indicating that the PAAS/CS coating from our study was more suitable for fruits with morphological changes than the CMC/CS coating.

#### Antimicrobial properties of PAAS/CS coating

Figure 3(D) shows the antibacterial effect of the PAAS/CS coating towards four foodborne pathogens. The highest antibacterial activity of the PAAS/CS coating was towards *E. coli* ( $99.6\%$ ), followed by *L. monocytogenes* and *Sal. Typhimurium* at  $98.5$  and  $92.6\%$ , respectively. In addition, the antibacterial effect of the coating towards *Sta. aureus*

was  $87.5\%$ . Therefore, the PAAS/CS coating displayed a good antibacterial activity on Gram-positive and Gram-negative pathogenic bacteria. Some previous works confirmed the antibacterial effects of applied modified CS coating against bacteria and fungi. This is mainly because the outermost layer of CS in the PAAS/CS coating contains partially positively charged amino groups, which can interact with the negative charges on the surface of the pathogenic bacteria by electrostatic attraction, causing the lysis of the bacterial cells (Hernández-Muñoz *et al.*, 2006; Perdones *et al.*, 2016; Zavareh *et al.*, 2020).

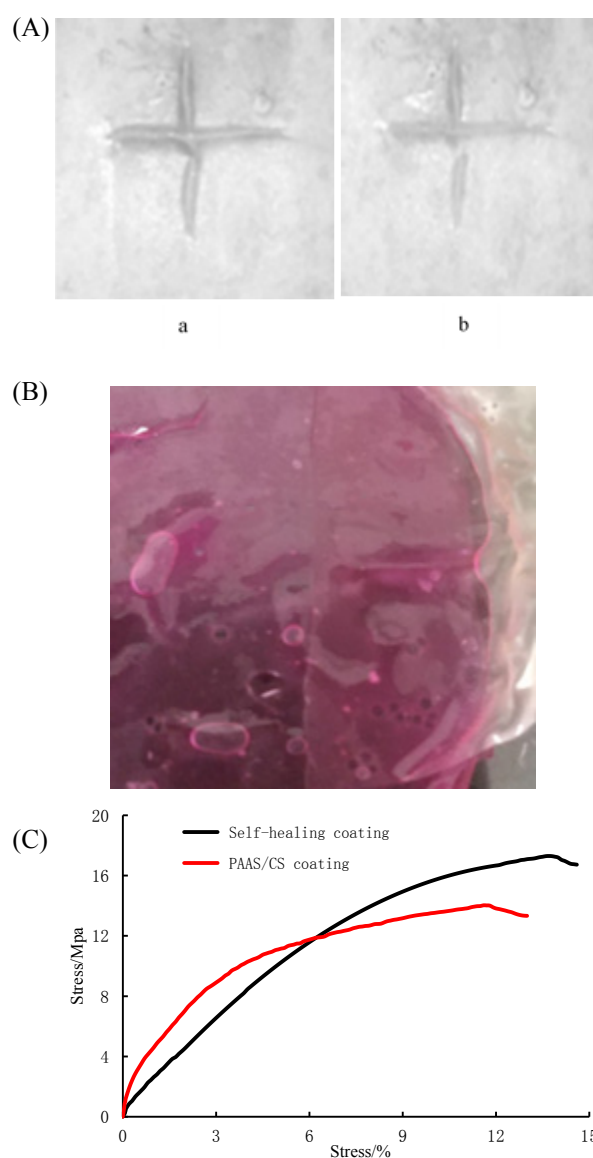


Figure 4. Self-healing results of PAAS/CS coating. (A) Microscopic self-healing results of PAAS/CS coating, and (B) Macroscopic self-healing results of PAAS/CS coatings. Note: (a) Coating scratches; and (b) Coating scratches after 30 min.

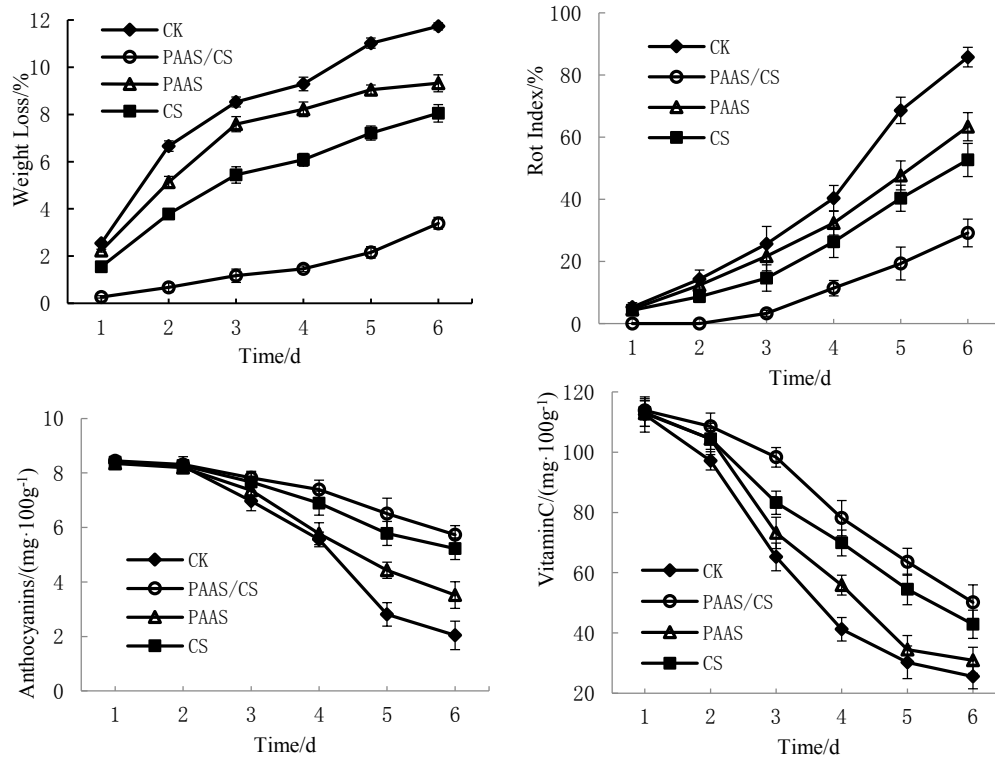


Figure 5. Fresh-keeping effect of PAAS/CS coating on strawberries. CK: uncoated group; PAAS/CS: coating with PAAS/CS group; PAAS: coating with PAAS group; CS: coating with CS group.

#### Self-repairing ability of PAAS/CS coating

##### Microscopic analysis of the self-repairing ability of PAAS/CS coating

The coating was scratched at the surface, and then covered with water, and observed under a microscope. The self-repairing results are shown in Figure 4(A). After 30 min, the scratch of the coating had become shallower, which indicated that the PAAS/CS coating has a strong self-repairing ability under the stimulating effect of water.

##### Macroscopic analysis of self-repairing abilities of PAAS/CS coatings

We also macroscopically analysed the self-repairing properties of PAAS/CS coatings. When two differently coloured coatings were placed in overlapping fashion for 30 min, a stable new self-repaired coating had formed (Figure 4(B)). We measured the mechanical properties of the new self-repaired coating and found that the TS was 14.03 MPa, which was only slightly lower than the TS (17.31 MPa) of the original PAAS/CS coating.

Based on the above results, we found that the self-repairing abilities of the PAAS/CS coating were manifested both by the repairing of the coating morphology, as well as by the mechanical properties. Liu *et al.* (2016) reported that this is mainly due to damage to the ionic bond in the damaged area upon scratching the coating, and the formation of a large

number of active groups on the surface of the coating. These reactive groups have good molecular mobility when in contact with water, allowing the formation of new hydrogen bonds and ionic bonds with other parts of the coatings in the water, leading to repair of the damaged area.

##### The effect of PAAS/CS coating on the storage and preservation of strawberries

Figure 5 shows that PAAS/CS coating improves the storage and preservation of strawberries. During storage, the weight loss and rot index of strawberries in the PAAS/CS group were significantly lower ( $p < 0.05$ ) than in the CK group. Moreover, after two days, the vitamin C and anthocyanin contents in the PAAS/CS group were also significantly higher ( $p < 0.05$ ) than in the CK group. As reported by Hernández-Muñoz *et al.* (2006), strawberries were treated either with 1% calcium gluconate dips, 1.5% chitosan coatings, or with a coating formulation containing 1.5% chitosan + 1% calcium gluconate and stored at 20°C for up to four days. When the surface of strawberries is covered by a PAAS/CS coating, the strawberries are prevented from being directly exposed to the air. The storage and preservation of strawberries can be improved by reducing the loss of moisture via the surface of the strawberry and by reducing the loss of nutrients. Perdonés *et al.* (2016) also reported that

coatings affected the metabolic pathways and volatile profile of fruits, and chitosan coatings containing lemon essential oils were described as effective at preventing the growth of fungi on fruit.

### Conclusion

Our results showed that when the concentration of PAAS was 5 mg/mL and that of CS was 9 mg/mL, CS and PAAS were uniformly distributed, and hydrogen and ionic bonds were assembled to form a relatively flat coating. Moreover, there was no apparent pore structure in the coating which was characterised by a tight cross-sectional structure. Under this condition, the PAAS/CS self-assembled layer displayed a higher water-resistance and transparency, which was highly suitable as a coating for the preservation of fruits. PAAS/CS coating displayed excellent mechanical properties and a strong bactericidal effect on Gram-positive and Gram-negative pathogens. The self-repairing ability of the PAAS/CS coating was characterised by repairing the morphology of the coating as well as the repairing of mechanical properties. The PAAS/CS coating significantly reduced the weight loss and rot index of strawberries during storage and preservation. At the same time, the loss of anthocyanin and vitamin C was also reduced, thus improving further the preservation of strawberries during storage.

### Acknowledgement

The present work was financially supported by Food Enzymatic Processing Technology Innovation Team of Chuzhou University (00001702), Science and Technology Program of Chuzhou (2018ZN019), Major Science and Technology Project of Anhui (18030701165), and Natural Science Research Project of Anhui Education Department (KJ2019A0638).

### References

Abugoch, L., Tapia, C., Plasencia, D., Pastor, A. and Escalona, V. H. 2015. Shelf-life of fresh blueberries coated with quinoa protein/chitosan/sunflower oil edible film. *Journal of the Science of Food and Agriculture* 96(2): 619-626.

American Society for Testing and Materials (ASTM). 1995. E96-95: standard test methods for water vapor transmission of materials. United States: ASTM.

American Society for Testing and Materials (ASTM). 2002. D882-02: standard test method for tensile properties of thin plastic sheeting.

United States: ASTM.

Arifin, H. R., Setiasih, I. S. and Hamdani, J. S. 2013. Shelf life and characteristics of strawberry (*Fragaria nilgerensis* L.) coated by aloe vera-glycerol and packed with perforated plastic film. *Acta Horticulturae* 1011(1): 307-311.

Arnon, H., Granit, R., Porat, R. and Poverenov, E. 2015. Development of polysaccharides-based edible coatings for citrus fruits: a layer-by-layer approach. *Food Chemistry* 166(1): 465-472.

Buchweitz, M., Speth, M., Kammerer, D. R. and Carle, R. 2013. Stabilisation of strawberry anthocyanins by different pectins. *Food Chemistry* 141(3): 2998-3006.

China Quality and Technical Supervision. 2000. GB/T 1038-2000: Plastics - film and sheeting - determination of gas-transmission rate -differential-pressure methods. China: China Quality and Technical Supervision.

Falk, K., Lindman, B., Bengmark, S., Larsson, K. and Holmdahl, L. 2001. Sodium polyacrylate potentiates the anti-adhesion effect of a cellulose-derived polymer. *Biomaterials* 22(16): 2185-2190.

Fasihnia, S. H., Peighambaroust, S. H. and Peighambaroust, S. J. 2018a. Nanocomposite films containing organoclay nanoparticles as an antimicrobial (active) packaging for potential food application. *Journal of Food Processing and Preservation* 42(2): article ID e13488.

Fasihnia, S. H., Peighambaroust, S. H., Peighambaroust, S. J. and Oromiehie, A. 2018b. Development of novel active polypropylene based packaging films containing different concentrations of sorbic acid. *Food Packaging and Shelf Life* 18: 87-94.

González Sandoval, D. C., Luna Sosa, B., Martínez-Ávila, G. C. G., Rodríguez Fuentes, H., Avendaño Abarca, V. H. and Rojas, R. 2019. Formulation and characterization of edible films based on organic mucilage from Mexican *Opuntia ficus-indica*. *Coatings* 9(8): article ID 506.

Helander, I. M., Nurmiäholassila, E. L., Ahvenainen, R., Rhoades, J. and Roller, S. 2001. Chitosan disrupts the barrier properties of the outer membrane of Gram-negative bacteria. *International Journal of Food Microbiology* 71(2): 235-244.

Hernández-Muñoz, P., Almenar, E., María-José, O. and Gavara, R. 2006. Effect of calcium dips and chitosan coatings on postharvest life of strawberries (*Fragaria × ananassa*). *Postharvest Biology and Technology* 39(3): 247-253.

- Hoque, M. S., Benjakul, S. and Prodpran, T. 2011. Properties of film from cuttlefish (*Sepia pharaonis*) skin gelatin incorporated with cinnamon, clove and star anise extracts. *Food Hydrocolloids* 25: 1085-1097.
- Hou, D., Zhang, G. and Pant, R. 2016. Micromechanical properties of nanostructured clay-oxide multilayers synthesized by layer-by-layer self-assembly. *Nanomaterials* 6(11): 204-211.
- Jiang, F., Yang, Y., Weng, J. and Zhang, X. 2016. Layer-by-layer self-assembly for reinforcement of aged papers. *Industrial and Engineering Chemistry Research* 55(40): 10544-10554.
- Kim, D. M., Yu, H. C., Yang, H. I., Cho, Y. J., Kwangmyong, L. and Chung, C. M. 2017. Microcapsule-type self-healing protective coating for cementitious composites with secondary crack preventing ability. *Materials* 10(2): 114-121.
- Kumarasamy, J., Camarada, M. B., Venkatraman, D., Ju, H., Dey, R. S. and Wen, Y. 2018. One-step coelectrodeposition-assisted layer-by-layer assembly of gold nanoparticles and reduced graphene oxide and its self-healing. *Nanoscale* 10(3): 1196-1206.
- Lee, J., Durst, R. W. and Wrolstad, R. E. 2005. Determination of total monomeric anthocyanin pigment content of fruit juices, beverages, natural colorants, and wines by the pH differential method: collaborative study. *Journal of AOAC International* 88(5): 1269-1278.
- Li, C., Li, J. A., Chang, J. W., Shi, B. J., Di, W. U. and Hao, H. Y. 2018. Mg-Zn-Y-Nd coated with citric acid and dopamine by layer-by-layer self-assembly to improve surface biocompatibility. *Science China Technological Sciences* 61(8): 1288-1237.
- Liu, X., Ren, J. and Zhu, Y. 2016. The preservation effect of ascorbic acid and calcium chloride modified chitosan coating on fresh-cut apples at room temperature. *Colloids and Surfaces A - Physicochemical and Engineering Aspects* 502: 102-106.
- Marelli, B., Brenckle, M. A., Kaplan, D. L. and Omenetto, F. G. 2016. Silk fibroin as edible coating for perishable food preservation. *Scientific Reports* 6(10): 25263-25270.
- Nottagh, S., Hesari, J., Peighambari, S. H., Rezaei-Mokarram, R. and Jafarizadeh, H. 2018. Development of a biodegradable coating formulation based on the biological characteristics of the Iranian ultra-filtrated cheese. *Biologia* 73(4): 403-413.
- Nottagh, S., Hesari, J., Peighambari, S. H., Rezaei-Mokarram, R. and Jafarizadeh-Malmiri, H. 2019. Effectiveness of edible coating based on chitosan and natamycin on biological, physico-chemical and organoleptic attributes of Iranian ultra-filtrated cheese. *Biologia* 75(3): 1-7.
- Odriozola, S. I., Soliva F. R. and Olga, M. B. 2008. Phenolic acids, flavonoids, vitamin C and antioxidant capacity of strawberry juices processed by high-intensity pulsed electric fields or heat treatments. *European Food Research and Technology* 228(2): 239-248.
- Perdones, A., Escriche, I., Chiralt, A. and Vargas, M. 2016. Effect of chitosan-lemon essential oil coatings on volatile profile of strawberries during storage. *Food Chemistry* 197: 979-986.
- Pinto, T. D. S., Alves, L. A., Cardozo, G. D. A., Munhoz, V. H. O., Verly, R. M., Pereira, F. V. and Mesquita, J. P. D. 2017. Layer-by-layer self-assembly for carbon dots/chitosan-based multilayer: morphology, thickness and molecular interactions. *Materials Chemistry and Physics* 186: 81-89.
- Sakooei-Vayghan, R., Peighambari, S. H., Hesari, J. and Peressini, D. 2019. Effects of osmotic dehydration (with and without sonication) and pectin-based coating pretreatments on functional properties and color of hot-air dried apricot cubes. *Food Chemistry* 311: article ID 125978.
- Sun, D. Q., Liang, G. B., Xie, J. H., Lei, X. and Mo, Y. 2010. Improved preservation effects of litchi fruit by combining chitosan coating with ascorbic acid treatment during postharvest storage. *African Journal of Biotechnology* 9(22): 3272-3279.
- Ugur, S., Sarışik, M. and Türkoğlu, G. 2016. Layer by layer assembly of antibacterial inclusion complexes. *International Journal of Clothing Science and Technology* 28(3): 368-377.
- Wang, H. and Zhou, Q. 2018. Evaluation and failure analysis of linseed oil encapsulated self-healing anticorrosive coating. *Progress in Organic Coatings* 118: 108-115.
- Wang, Y., Ding, X., Chen, X., Chen, Z., Zheng, K. and Chen, L. 2017. Layer-by-layer self-assembly photocatalytic nanocoating on cotton fabrics as easily recycled photocatalyst for degrading gas and liquid pollutants. *Cellulose* 24(10): 4569-4580.
- Widiastuti, A., Yoshino, M., Saito, H., Maejima, K., Zhou, S. Y., Odani, H., ... and Sato, T. 2013. Heat shock-induced resistance in strawberry against crown rot fungus *Colletotrichum*

- gloeosporioide*. Physiological and Molecular Plant Pathology 84: 86-91.
- Xu, S., Chen, X. and Sun, D. W. 2001. Preservation of kiwifruit coated with an edible film at ambient temperature. Journal of Food Engineering 50(4): 211-216.
- Yang, F., Wang, P., Yang, X. and Cai, Z. 2017. Antifogging and anti-frosting coatings by Dip-layer-by-layer self-assembly of just triple-layer oppositely charged nanoparticles. Thin Solid Films 634: 85-89.
- Zavareh, S. A. H. T. and Ardestani, F. 2020. Antibacterial effects of chitosan coating containing *Mentha aquatica* L. essence against *Escherichia coli*, *Staphylococcus aureus* and *Listeria monocytogenes* in Iranian white cheese. International Journal of Dairy Technology 70: 1-12.
- Zhang, R., Chen, Z. Y., Fang, G. Z., Ma, Y. M. and Dai, X. F. 2009. Immobilization of  $\beta$ -galactosidase on carboxymethyl cellulose-chitosan polyelectrolyte complex. Chemistry and Industry of Forest Products 29(10): 138-142.
- Zhao, N., Yang, Z., Wang, Y., Zhao, B., Bian, F., Li, X. and Wang, J. 2016. Probing the surface microstructure of layer-by-layer self-assembly chitosan/poly(L-glutamic acid) multilayers: a grazing-incidence small-angle X-ray scattering study. Materials Science and Engineering C 58: 352-358.
- Zhao, Y., Zhang, Z., Shi, L., Zhang, F. and Zeng, R. 2019. Corrosion resistance of a self-healing multilayer film based on SiO<sub>2</sub> and CeO<sub>2</sub> nanoparticles layer-by-layer assembly on Mg alloys. Materials Letters 237(15): 14-18.